

# Lubricant Degradation and Related Wear of a Steel Pin in Lubricated Sliding Against a Steel Disc

Archana Singh,<sup>†</sup> Ravi T. Gandra,<sup>†</sup> Eric W. Schneider,<sup>‡</sup> and Sanjay K. Biswas<sup>\*,†</sup>

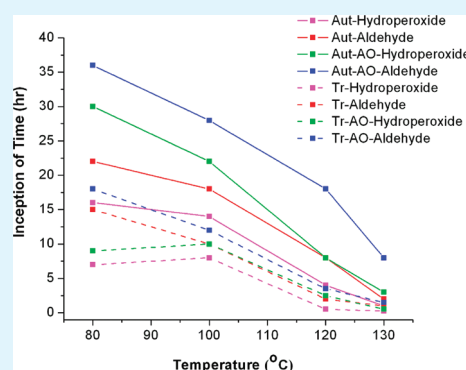
<sup>†</sup>Nanotribology Lab, Department of Mechanical Engineering, Indian Institute of Science, Bangalore 560 012, India

<sup>‡</sup>Chemical Science and Materials Systems Laboratory, General Motors Research and Development Centre, 30500 Mound Road, Warren, Michigan 48090, United States

## S Supporting Information

**ABSTRACT:** In lubricated sliding contacts, components wear out and the lubricating oil ages with time. The present work explores the interactive influence between lubricant aging and component wear. The flat face of a steel pin is slid against a rotating steel disk under near isothermal conditions while the contact is immersed in a reservoir of lubricant (hexadecane). The chemical changes in the oil with time are measured by vibrational spectroscopy and gas chromatography. The corresponding chemistry of the pin surface is recorded using X-ray photoelectron spectroscopy while the morphology of the worn pins; surface and subsurface, are observed using a combination of focused ion beam milling and scanning electron microscopy. When compared to thermal auto-oxidation of the lubricant alone, steel on steel friction and wear are found to accentuate the decomposition of oil and to reduce the beneficial impact of antioxidants. The catalytic action of nascent iron, an outcome of pin wear and disk wear, is shown to contribute to this detrimental effect. Over long periods of sliding, the decomposition products of lubricant aging on their own, as well as in conjunction with their products of reaction with iron, generate a thick tribofilm that is highly protective in terms of friction and wear.

**KEYWORDS:** oil oxidation, tribology, reaction kinetics, antioxidant, steel



## 1. INTRODUCTION

By the early 1990s a definitive understanding of the auto-oxidation of hydrocarbonaceous oils had been reached. The reaction kinetics have been formulated<sup>1–6</sup> on the basis of experimentation. Unstable hydroperoxides<sup>6,7</sup> form slowly as primary products of hydrocarbons, over an induction time,<sup>2,3</sup> by hydrogen abstraction.<sup>2,6,8,9</sup> The concentration of hydroperoxide reaches a maximum at which times the hydroperoxides are converted to carbonyl (C=O) functions, alcohols, and new alkyl radicals.<sup>5</sup> The carbonyl functions are aldehydes, ketones, esters and carboxylic acids<sup>6</sup> while the alkyl radicals yield peroxy radicals which propagate the reactions.<sup>10</sup> The aldehydes, ketones and alcohols may be further oxidized to give carboxylic acids.<sup>10</sup> The decomposition of hydroperoxide that leads to their depletion and the consequent yield of carbonyl function products occurs rapidly.<sup>5</sup> Here we benchmark oxidation inception of hexadecane by the first appearance of the carbonyl peak, as measured by FTIR spectroscopy.<sup>4,5</sup>

Antioxidants are added to hydrocarbons to inhibit lubricant oxidation. Most antioxidant additives either react with peroxy radicals to form a less reactive radical and a hydroperoxide or they decompose hydroperoxide to form molecular, rather than free radical products.<sup>6</sup> Plaza<sup>11,12</sup> has shown that the alkyl radicals in oil react with organic disulfide antioxidants to give elemental sulfur, thiols, organic sulfides, and hydrogen sulfide.

In summary, auto-oxidation and chemical changes in the oil used to lubricate steel on steel sliding contacts have been studied and the reaction kinetics of alkyl disulfide antioxidants in auto-oxidation and mechanical sliding contacts have been debated. The effect of the changes in bulk oil in sliding contacts on wear of components and the effect of wear on decomposition of oil have rarely<sup>13–16</sup> been investigated.

Aging of lubricant normally leads to a modest increase of viscosity with time. At a critical time when the reaction kinetics lead to the rapid formation of high-molecular-weight products, the increase in viscosity is catastrophic and engine performance is severely impaired.<sup>17</sup> The reaction kinetics are such that active radicals are perpetually released into oil. Generation of such radicals, apart from contributing to the increase of viscosity, on the one hand, is likely to be influenced catalytically by the presence and attrition of<sup>10,18</sup> iron-based engine components. On the other hand the decomposition products are likely to react with such components in altering their surface properties, which may result in changes in friction and wear of such components.

In this paper, we first record the changes in decomposition of lubricating oil due to steel-on-steel sliding contact, distinct from

Received: March 25, 2011

Accepted: June 17, 2011

Published: June 17, 2011

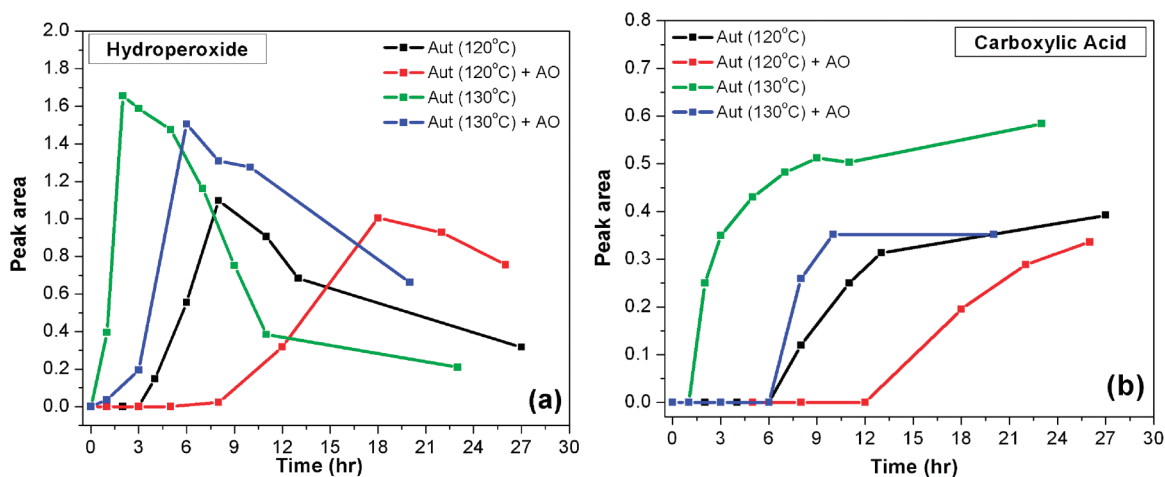


**Figure 1.** Oxidative product growth for auto-oxidative degradation of hexadecane with and without antioxidant additive (DMDS) at 120 and 130 °C.

those due to auto-oxidation. Given such changes in the oil, we explore corresponding surface modifications of a steel pin rubbing a steel disk under lubricated condition in a pin-on-disk machine. The data enables us to rationalize the transient and steady state phases of the wear of the pin. The lubricant used is hexadecane, the mean contact pressure is 1.76 MPa, and the sliding speed is 0.52 m/s.

## 2. EXPERIMENTAL SECTION

**2.1. Materials.** The model base fluid used in all the experiments was *n*-hexadecane (>99%), supplied by Sigma-Aldrich Inc. Dimethyl disulfide (DMDS) (>99%), supplied by Merck, Germany, was used as the antioxidant additive. All chemicals were used without any further purification.

**2.2. Tests.** **2.2.1. Auto-oxidative Degradation of Oil.** Oil was heated in a 100 mL three-neck round-bottom flask fitted with a condenser and a thermometer. A controller with a feed back loop was used to maintain the oil at a constant temperature. The volume of oil was kept constant for all the experiments. An electrically operated stirrer was used to stir the oil at all times during an experiment. The oil temperature was varied between room temperature and 130 °C. The maximum duration of a test was 64 h.

The heated oil was collected at regular intervals, centrifuged and analyzed using Fourier Transform Infrared (FTIR) spectroscopy and gas chromatography–mass spectrometry (GC-MS).

The following tests were conducted: (1) pure hexadecane and (2) DMDS dispersed in hexadecane in 1% (v/v) ratio.

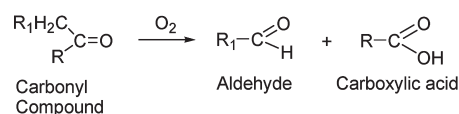
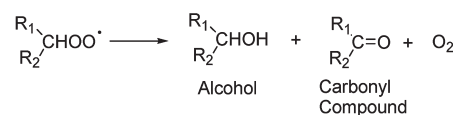
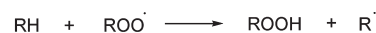
**2.2.2. Lubricated Sliding Interaction of Stationary Pin on Rotating Disk.** A schematic of a pin-on-disk tribometer (DUCOM, Bangalore, India) used in this study is given in the Supporting Information (Figure S1a). A 6 mm diameter pin was fixed to a holder at a 50 mm radius of the disk where a concentric groove of 34 mm width and 28 mm depth was machined a priori. The groove on the disk was flooded with 120 mL of the lubricating oil. A radiator heater kept in the central portion of the disk heated the disk to oil test temperature. The oil temperature in the groove was monitored manually periodically with a thermometer and the disk heater controller was adjusted to maintain oil temperature within  $\pm 2$  °C of the test temperature. The pin holder was heated using resistance coils, a thermocouple attached to the holder monitored the temperature and fed the data to a controller which maintained the pin at the same temperature of the oil using feed back loop. The sliding test conditions for all the experiments were: Normal load = 50 N (mean contact pressure = 1.76 MPa), sliding velocity = 100 rpm (surface speed = 0.52 m/s).

See the Supporting Information sections S2.3, which give the technical details of oil analysis by Fourier Transform infrared

spectroscopy (FTIR), gas chromatography–mass spectrometry (GC-MS). Supporting Information S2.4, gives the technical details of surface and subsurface study by scanning electron microscopy (SEM), focused ion beam (FIB) milling, X-ray photoelectron spectroscopy (XPS), energy-dispersive X-ray Spectroscopy (EDS), and optical profilometry.

## 3. RESULTS AND DISCUSSION

The auto-oxidation of hexadecane at 120 and 130 °C as shown in panels a and b in Figure 1 are more or less as expected. See Figure S2a–c in the Supporting Information for oxidation products alcohol, aldehyde, and ketone. Oxidation of oil to an alkyl hydroperoxide to a peak concentration is followed by slow depletion of the ROOH in time. As the oil is oxidized hydroperoxide accumulates to a peak concentration<sup>10</sup> which in time coincides with the peak of the oxygen uptake rate. Subsequently as this rate declines accumulation of ROOH slows down significantly even though hydrocarbon (RH) is available to react with oxygen as shown by the GC-MS analysis data of used oil (see the Supporting Information, Figure S3). The ROOH accumulated at the peak concentration decomposes with time by autoacceleration. After the ROOH concentration approaches its maximum value, alcohols, aldehydes, ketones, and carboxylic acids appear as secondary reaction products.



The reason for the depletion of ROOH in oil (Figure 1a) beyond the peak concentration is that the characteristic reaction rates for the generation of secondary oxidation products are

higher than that for the production of hydroperoxides (primary oxidation product).<sup>6</sup> When the oil temperature  $T$  is 130 °C, the primary product ROOH starts to be generated within an hour after the commencement of heating. Reducing  $T$  from 130 to 120 °C delays the inception of ROOH generation, reduces the peak concentration, increases the time required for achievement of peak concentration from 2 to 8 h, and reduces the (time) gradient of concentration decay by about 3 times. The secondary products, carbonyl functions and alcohols, are incepted exactly when the ROOH peak concentration is achieved and their rate of generation slows down as the ROOH is depleted in time. The rate of secondary product generation reduces somewhat with decreasing oil temperature. Dispersion of antioxidant DMDS in oil heated to 120 and 130 °C delays the achievement of ROOH peak concentration and slows down the subsequent concentration decay. The secondary products inception follows the ROOH peak concentration time as is in the case when no antioxidant is added. The quantity of secondary product is significantly reduced when the antioxidant is used. The antioxi-

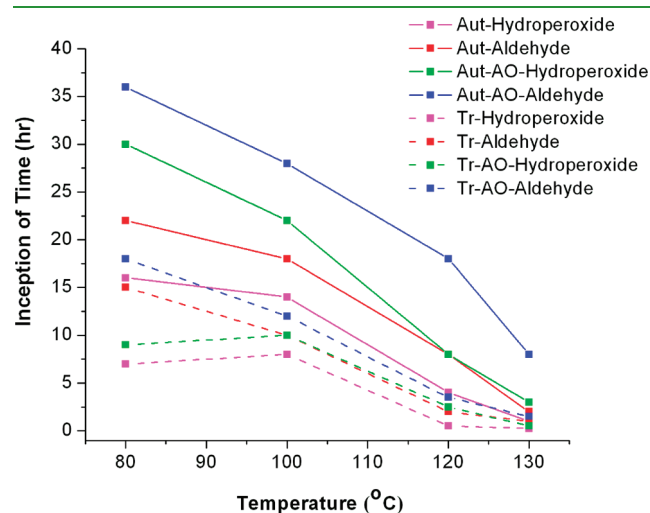


**Figure 2.** Inception time of different oxidative products. The inception time of alcohol, aldehyde, ketone and carboxylic acid are identical. Thus only the aldehyde data are shown. — auto-oxidation (Aut), ---- tribo-oxidation (Tr). AO, DMDS antioxidant.

idant is more effective when the oil temperature is reduced to 120 °C. The rate of ROOH production slows down further and the inception time for secondary product is extended further, compared to what happens when the antioxidant is present in the oil heated to 130 °C. When the oil carrying the antioxidant is heated to 120 °C, the secondary products appear to be incepted before the ROOH peak concentration is achieved.

When sliding experiments (tribo-oxidation) are conducted with hexadecane heated to the same temperature as in the auto-oxidation experiments, the inception times for carbonyl functions (Figure 2) are significantly less than those corresponding to the auto-oxidation experiments. Figure 2 shows that the inception times of auto-oxidation and tribo-oxidation are well separated at low temperatures and they converge with increasing oil temperature. The secondary products of tribology as reported in Figure 2 using FTIR spectroscopy were confirmed by GC-MS analysis of the oil extracted from tribological experiments. The GC-MS analysis of the oil (not shown) extracted after 1 h 45 min of sliding interaction yielded traces of alcohols, aldehydes, and hexadecane isomers. The GC-MS analysis of the oil extracted from the tribological experiment after 9 h of sliding however show a firm presence of aldehydes, alcohols and carboxylic acids. For the details of this analysis, see the Supporting Information, Figure S3. The alcohol and carbonyl function are of varying chain length in the  $C_5$ – $C_{15}$  range (lower than  $C_{16}$  of the parent hexadecane). The oxidized compounds present before 18.9 min retention time (hexadecane) are straight chain alcohol, aldehyde and carboxylic acid compounds (see the Supporting Information Figure S3). After 18.9 min retention time, straight chain as well as branched compounds are detected (see the Supporting Information, Figure S3). In the absence of additive, 29% of hexadecane gets oxidized after 6 h of running. In the presence of antioxidant, 27% of the oil gets oxidized after 9 h of running. All the oxidized products are potentially triboactive compounds, which can react with iron on the sliding surface.

The distinction between auto-oxidation and tribo-oxidation as they give rise to primary and secondary products of oil decomposition is explored below in detail by FTIR spectroscopy of hexadecane heated to 80° and 120 °C.

Comparing the auto-oxidation and tribo-oxidation data in panels a and b in Figure 3, it is clear that in the two cases: (i) the rates of depletion of the hydroperoxide are different, (ii) the rate

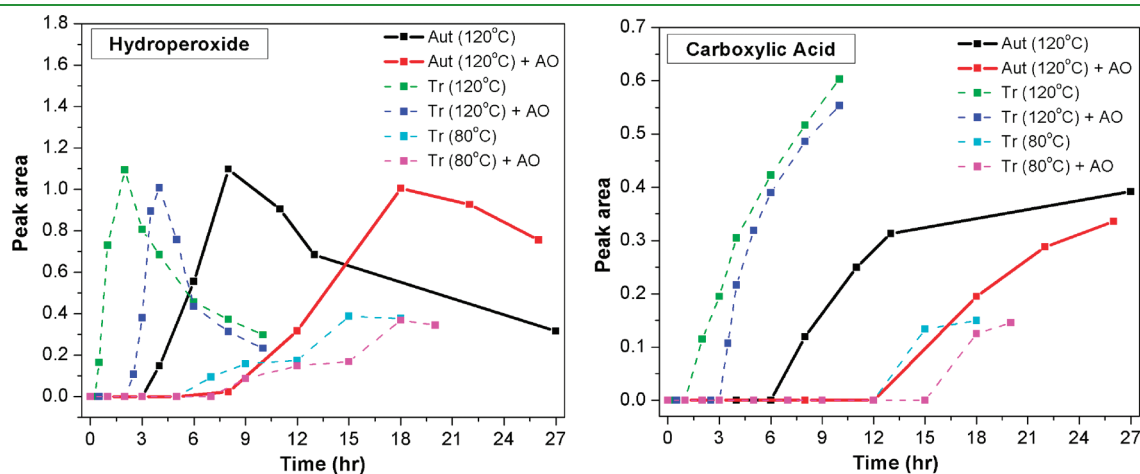


**Figure 3.** Oxidative product growth, comparing auto-oxidative and tribo-oxidative degradation of hexadecane with and without additive at 80 and 120 °C. AO, DMDS antioxidant; Aut, auto-oxidation; Tr, tribo-oxidation.

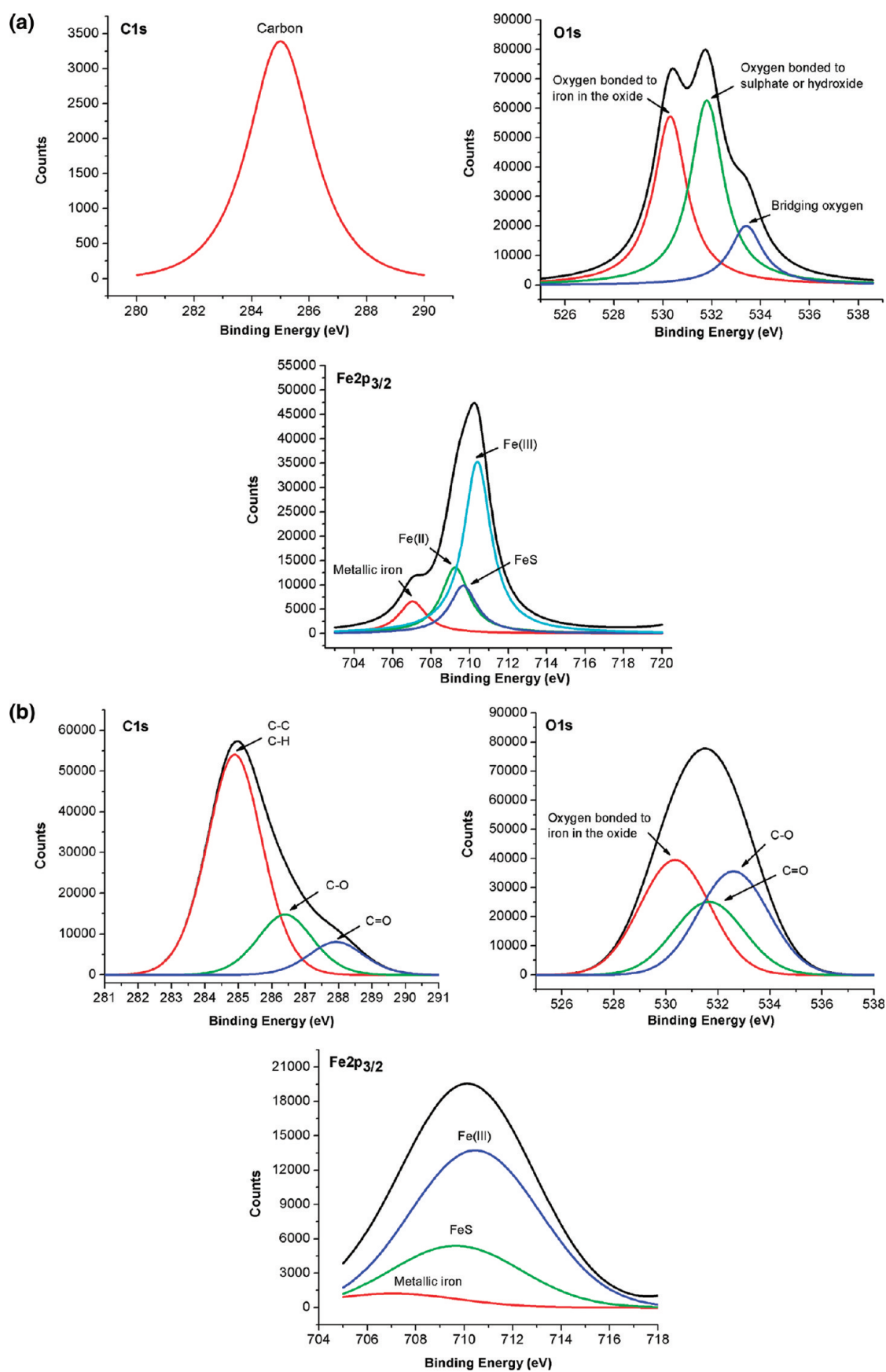
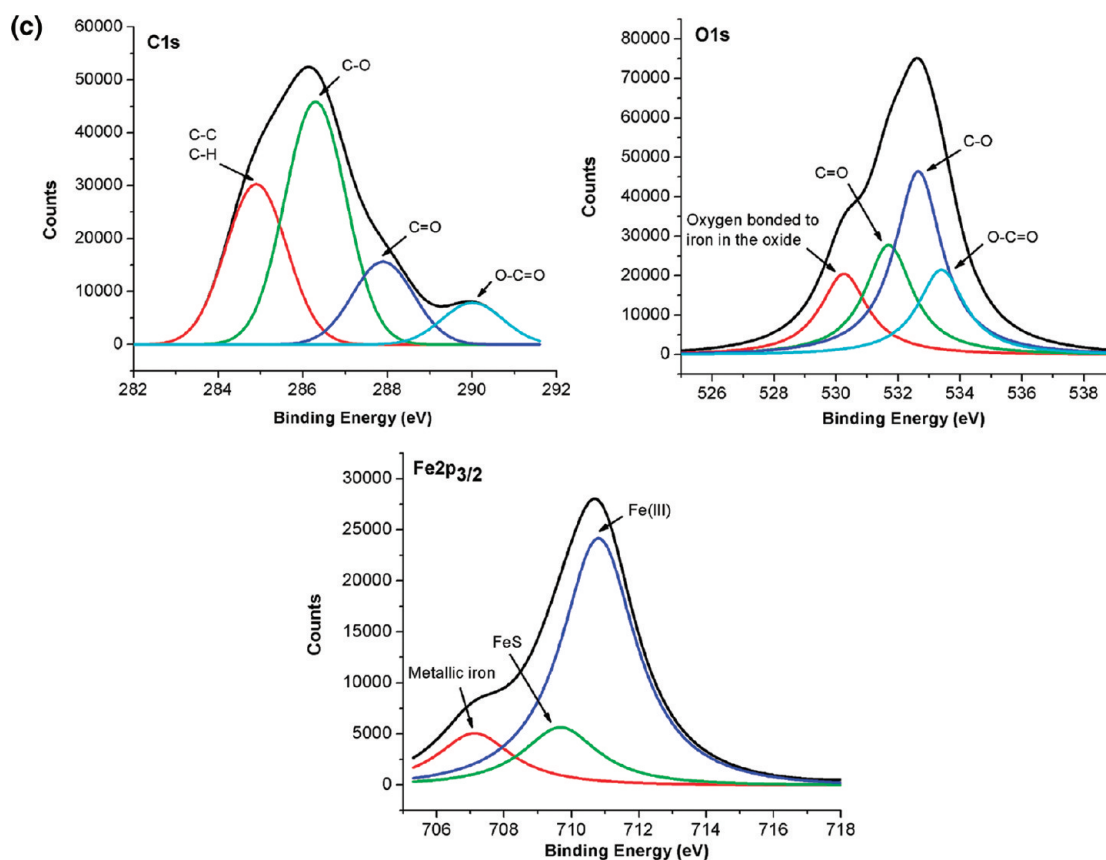


Figure 4. Continued

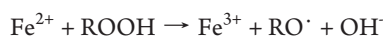
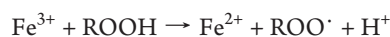




**Figure 4.** XPS detail spectra of C1s, O1s, and Fe $2p_{3/2}$  of steel pin with additive at 130 °C and 30 min (top three), 1 h 45 min (middle three) and 9 h (bottom three) of sliding time.

of generation of the carbonyl functions follow the rates of ROOH depletion, and (iii) the rate of hydroperoxide depletion in tribo-oxidation is very high initially compared to that in auto-oxidation. See Figure S4a–c in the Supporting Information for oxidation products alcohol, aldehyde, and ketone. The FTIR results (peak area estimation) shows that the tribo-oxidation in aggregate generates 30% more carbonyl function molecules than what is generated by auto-oxidation alone, even when the oil in both cases are heated to the same temperature. The decomposition processes for auto-oxidation and tribo-oxidation are the same qualitatively, although their process kinetics (reaction rates) are significantly different.

A possible reason for this difference between the process kinetics of auto-oxidation and tribo-oxidation is the catalytic action of soluble iron, which gives rise to unstable peroxy radicals. Colelough<sup>18</sup> suggests the following catalytic reactions



Colelough<sup>18</sup> and Naidu<sup>19</sup> find the presence of soluble iron as in organometallic complexes, to take part in catalytic action of Fe<sup>3+</sup> to degrade oil. The insoluble iron oxide Fe<sub>2</sub>O<sub>3</sub> is also known<sup>20</sup> to act as a catalyst to generate excess radicals. With reference to the XPS data of the pin shown in Figure 4a, a large peak at 710.7 eV may be attributed to Fe<sup>3+</sup> as in Fe<sub>3</sub>O<sub>4</sub>, FeOOH, and Fe<sub>2</sub>O<sub>3</sub>.

Makawoha<sup>14</sup> suggests that a peak at 711.3 eV is typical of an Fe–O bond present in compounds such as iron carboxylate.

XPS data also provide evidence for the buildup of carbon containing compounds on the pin surface during tribo-oxidation. Compared to what is achieved (2–3% C) in the first 30 min to 1 h of sliding (Table 1), Table 2 (tribo-oxidation after 1 h 45 min) shows the presence of a large amount (45–55% C) on the pin surface. The carbon is present in C=O, C–O, and C–H bonds (Figure 4- tribo-oxidation after 1 h 45 min). Kajdas<sup>13</sup> suggests that the C–O bond indicates the presence of iron carboxylate. Figure 4 (tribo-oxidation after 9 h) shows the presence of carboxylic acid in the oil. It is in fact suggested that tribology generates iron–carboxylate soap,<sup>13,14</sup> which is soluble in oil.

The foregoing discussion suggests that as the sliding interactions between two steel surfaces result in wear, fresh and reactive (oxygen donor) metal surfaces are continuously exposed to the lubricant.<sup>13</sup> A condition is created, especially when the oil is heated, for the creation of compounds of iron, oxygen, and carbon, which act as catalysts for oxidation of the oil in excess of what will be achieved by a stable thermal decomposition of hydroperoxide.

To highlight the catalytic action of iron in the oxidation of oil, we performed sliding wear experiments where all other materials and conditions remaining the same, the steel pin is replaced by a pure aluminum pin of the same dimension as the steel pin. Aluminum compared to iron is noncatalytic for organic reactions. Figure 5 shows that changing the pin from steel to aluminum

**Table 1. Atomic Weight Concentration (%) of the Elements on the Steel Pin Surface in Stage I, As Determined Quantitatively from the XPS Spectra, and As a function of Time in Tribo-oxidation of Hexadecane at 130 °C**

		element (at %)			
sliding time		C	O	Fe	S
without additive	30 min	2.3	88.0	9.7	
	1 h	3.4	81.9	14.7	
with additive	30 min	1.3	86.26	12.3	0.14
	1 h	2	79.95	17.8	0.25

		without additive (element (at %))		with additive (element (at %))	
sliding time		Fe (II)	Fe (III)	Fe (II)	Fe (III)
stage I	30 min	2.67	4.1	2.8	4.6
	1 h	3.45	6.91	2.21	8.84
stage II	1 h 45 min (105 min)	0	4.5	0	6.1
stage III	6 h (360 min)	0	4.1		
	9 h (540 min)			0	4.5

**Table 2. Atomic Weight Concentration (%) of the Elements on the Steel Pin Surface in Wear Stage II at 130 °C Temperature**

		element (at %)			
sliding time		C	O	Fe	S
without additive	1 h 45 min	53.4	41.3	5.3	
with additive	1 h 45 min	46.54	44.5	8.9	0.06

delays the inception of the hydrogen peroxide generation by 6 h, delays the inception of secondary products by 9 h and the quantities of peroxide and carbonyl products generated are also reduced significantly. The generation of other oxidation products, alcohol and aldehyde, is given in the Supporting Information, Figure S5.

Comparing the results of the above two experiments (Figure 5), it has to be noted that the discs in both the experiments are the same and made of steel. It is the replacement of the steel pin by an aluminum pin which brings about a dramatic reduction in the oxidation of oil. From this, we infer that it is the surface of the steel pin (which is continuously rubbed and not a point on the disk surface which is rubbed only once in a revolution) that is responsible for providing the catalytic action for the fast (at oil/pin/disk temperatures more than 100 °C) oxidation/decomposition of the oil.

Savage and Blaine<sup>5</sup> suggest another route for the formation of carbonyl functions where carboxylic acids can form directly by  $\alpha$ ,  $\gamma$  cleavage of hydroperoxy ketones and direct oxidation of aldehydes by  $\beta$ -scission of alkoxy radicals. The alkoxy radicals may also abstract hydrogen directly to form alcohols. These possible routes which bypass the decomposition of hydroperoxides for producing carbonyl compounds have been noted in auto-oxidation studies of hexadecane. Their reaction rates in the presence of a reactive iron catalyst, as available in a sliding wear experiment, are not known to us.

We have observed in Figure 1 the dramatic delay in the degradation of oil: enhancement of oxidation inception time and reduction in the volume of secondary products, which may be achieved by adding (DMDS) antioxidant to the oil. This

mechanism is well understood.<sup>10,11</sup> The alkyl disulfide is a hydroperoxide decomposer that yields alcohols by breaking down the hydroperoxides while they themselves are oxidized to give sulfoxides or sulphones. The latter may break down further to sulfonic and sulphuric acids which on their own are hydroperoxide decomposers. It is interesting to note from Figure 3 that the advantage of oxidation inhibition by addition of antioxidant, observed in auto-oxidation, is practically lost when the oil is used for lubricating a steel–steel contact. The advantage is marginally recovered when the oil temperature is lowered. This is in contrast to the effectiveness (this will be shown later in the paper) of the antioxidant as an antiwear compound and a friction modifier.

The antioxidant slows down<sup>6</sup> oxidation of oil by ingesting alkyl hydroperoxides and peroxy radicals. When the hydroperoxide-antioxidant reaction is faster than the rate at which hydroperoxide decomposes, the antioxidant is effective. Figure 1 shows that the hydroperoxide decomposes very slowly in auto-oxidation. The antioxidant is thus very effective in slowing down the oxidation of oil even further (Figures 1 and 3). When the decomposition of ROOH however is very fast as in the sliding contact situation we may suggest that because of the catalytic action of nascent iron, the presence of Fe<sub>2</sub>O<sub>3</sub>, soluble organic-metallic compounds and/or peroxy radicals, the antioxidants are readily ingested. The finite quantity of antioxidant is depleted to allow subsequent generation and decomposition of hydroperoxide at rates as if no antioxidant is present. Figure 3 shows that the presence of antioxidant delays the generation of ROOH by 2 h in tribo-oxidation. After 2 h of ROOH depletion from the peak concentration, the concentration–time characteristic for ROOH is insensitive to the addition of antioxidant. The antioxidant however becomes marginally more effective in extending inception time (Figure 2) at lower oil temperatures.

Given the changes brought about by the steel-on-steel sliding action to the lubricating oil, we will address the consequence of such changes on the wear of the steel pin used in tribology. Figure 6 shows that there are three characteristic wear (pin displacement) rates. Each characteristic corresponds to a specific time period in the history of sliding; we mark them as stages I, II, and III. We have repeated these experiments four times and

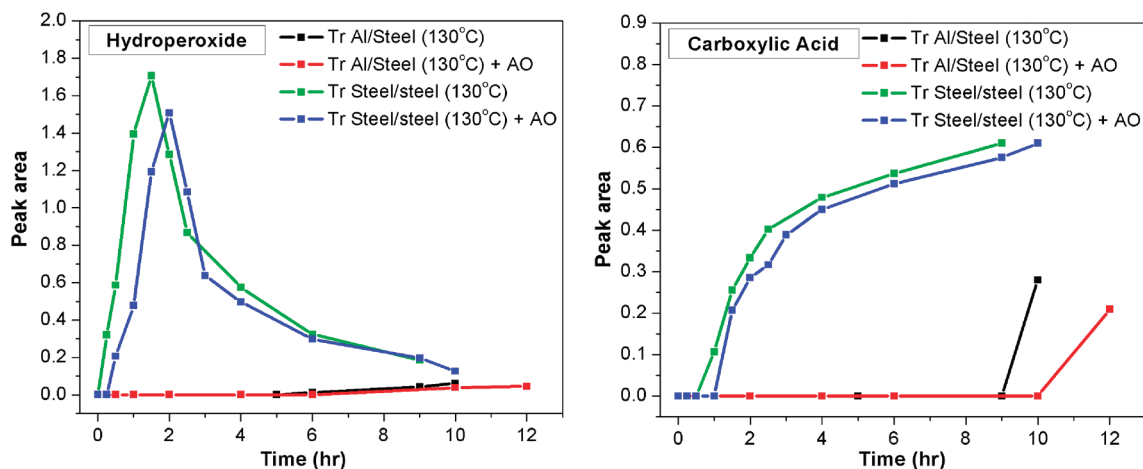


**Figure 5.** Oxidative product growth, comparing tribo-oxidative degradation of hexadecane with and without additive using steel/steel and Al/steel, pin/disk interactions at 130 °C.

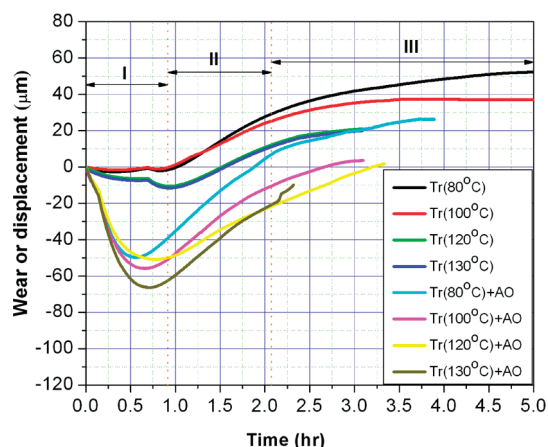


**Figure 6.** Plot of wear (displacement) as a function of time for tribo-oxidation of hexadecane with and without additive; downward movement of the pin surface corresponds to positive displacement.

found the trends repeatable. For clarity, we show representative data in Figure 6. Over a total sliding time of 10 h, however, we found in stage III a large scatter in the wear rate data, on the order of  $\sigma = \pm 1.5 \mu\text{m/h}$  around a mean of  $5 \mu\text{m/h}$ .

**Stage I:** When the oil temperature is 100 °C or less, there is negligible displacement of the pin. At higher temperatures the displacement is negative. Also, when the antioxidant additive is used, at all temperatures, the rate of displacement is negative. When the additive is employed, the negative displacement (the pin and the disk are moving away from each other) is significantly more than when there is no additive.

**Stage II:** The wear rate is strongly positive. When the additive is used, the wear rate is much higher than when no additive is used.

**Stage III:** The positive wear rate is less than what is observed in stage II. In the absence of the additive, the wear rate is high when the oil temperature is less than 100 °C.

We explore below the chemistry of the slid pin surface using X-ray photoelectron spectroscopy (XPS). Our purpose is to comment on whether and how oil aging influence wear.

**Stage I.** Figure 4a shows representative  $\text{C}_{1s}$ ,  $\text{O}_{1s}$  and  $\text{Fe}_{2p_{3/2}}$  XPS spectra of the surfaces of the pin slid with oil containing the

AO additive heated to 130 °C after 30 min (middle of stage I). Binding energy values of all the peaks were corrected by a charge correction factor corresponding to  $\text{C}_{1s}$  peak at 285 eV. The spectra show the presence of oxygen in different iron oxide compounds. Table 1 shows a negligible amount of carbon on the surfaces during stage I. Table 1 shows that in the absence of the antioxidant the concentration of both  $\text{FeO}$  (as given by  $\text{Fe}^{2+}$  peak) and  $\text{Fe}_3\text{O}_4$ ,  $\text{FeOOH}$  and  $\text{Fe}_2\text{O}_3$  (as given by  $\text{Fe}^{3+}$  peak) compounds increases with sliding time during stage I. When there is additive the intensity of the more stable  $\text{Fe}_3\text{O}_4$  and  $\text{Fe}_2\text{O}_3$  increases whereas that of  $\text{FeO}$  decreases with time.

We have shown (Figure 3) that in tribo-oxidation, DMDS only marginally inhibits oil oxidation. Further, considering that there is only a very small amount of C found on the slid surface in stage I, we argue that the antioxidant is readily available to be adsorbed on the iron surface to form, initially, thiolates by cleavage of the S–S bond and then  $\text{FeS}$  when the C–S bond is cleaved.<sup>21,22</sup> Table 1 shows that the sulfur concentration increases with time in stage I. It may be suggested that hydrocarbon aging plays no role in stage I wear. Stage I is characterized by the creation of films of oxides and sulfides that increase in thickness with time. The pin is lifted in the process showing a negative wear rate. When the antioxidant is used the film on both the pin and disk build up with time. At the end of 1 h of running, contact and noncontact profilometry data of the slid pin and disk respectively show a deposit of 6–8  $\mu\text{m}$  on both the surfaces. Such surface deposits with the debris present in the oil may account for the negative displacement of the pin seen in Figure 6. The availability of a large quantity of unoxidized disulfide may accentuate this process. At this stage thick layers of oxides and sulfides slide against each other creating conditions for low friction and low attrition.

Previous workers<sup>11,12</sup> have noted and rationalized the coexistence of iron oxide and iron iron sulphide when steel components mate and wear out in the presence of a hydrocarbon based lubricant containing disulfide antioxidants. For the relatively modest contact pressures used in the present investigation we believe that the generation of iron oxide discourages the generation of iron sulphide and the coexistence of oxide and sulphides of iron that we find in the tribofilm and on the pin surface is chemically justified. See a brief discussion of this phenomenon in the Supporting Information S3.



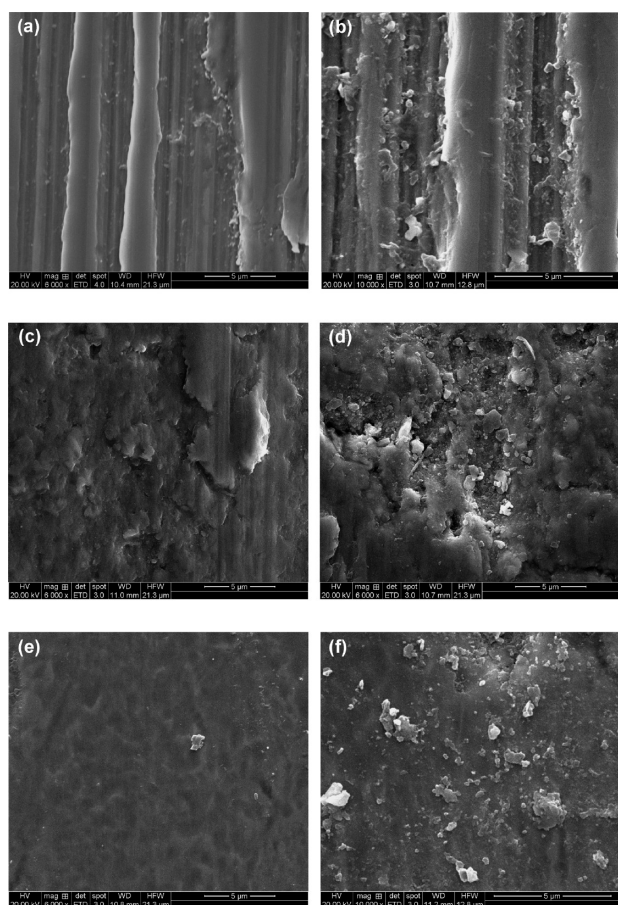


**Figure 7.** SEM micrographs of the steel pin sample lubricated by hexadecane at 80 °C temperature. (a) 1 h without AO, (b) 1 h 45 min without AO, (c) 1 h with AO (d) 1 h 45 min with AO, (e) 6 h without AO, and (f) 6 h with AO.

**Stage II.** Figures 2, 3, and 5 show that the carbonyl functions (aldehydes, ketones and carboxylic acids) and alcohols first appear in hexadecane after 1 h of sliding when  $T = 120$  °C and after 45 min of sliding when  $T = 130$  °C. Figure 6 shows that these times mark the end of stage I and beginning of stage II. Figure 4b shows representative XPS spectra of the surface of the pin slid in stage II. Signatures of C–H (alkyl), C–O (alcohol) and C=O (carbonyl) and FeS (absent when no additive is used) bonds appear in the spectra. The XPS spectra (not shown) of the pin surface lubricated without antioxidant exhibit the same peroxide decomposition products. Table 2, a quantitative summary of the XPS stage II spectrum, shows an abundance of carbon on the pin surface in stage II compared to what is observed in stage I (Table 1a). This clearly indicates that the decomposition of the lubricating oil starts in the stage II of the sliding process.

The oil decomposition is accompanied by a rapid wear (Figure 6) of the oxide and sulphide films generated in stage I. Figure 7 shows the evidence of a such attrition when the oil temperature is 80 °C. Figure 8a shows a 400 nm thick tribolayer, made up principally of oxide and sulphide of iron (see the Supportive Information, Table S1), which forms in stage I. Figure 8b shows the disappearance of this tribolayer in stage II accompanied by plastic flow and deformation of the subsurface, phenomena which indicate wear.

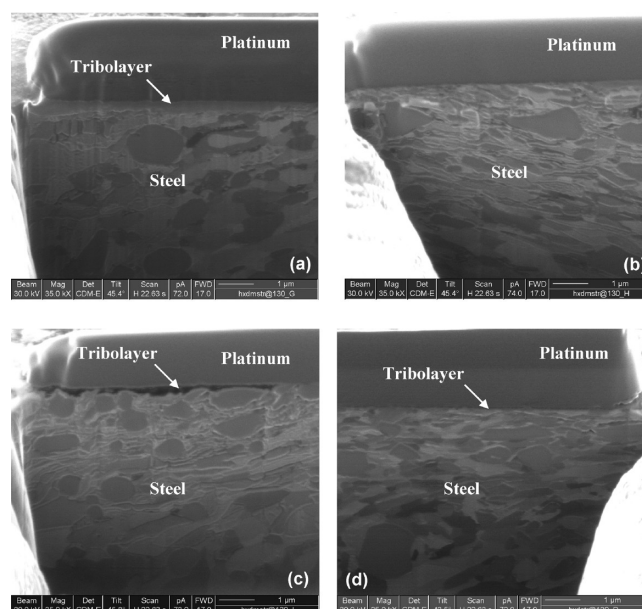


**Figure 8.** FIB images of the subsurface of pin sample showing tribolayer on steel surface (a) with antioxidant, 1 h (stage I); (b) with antioxidant, 1 h 45 min (stage II); (c) with antioxidant, 9 h (stage III), and (d) without antioxidant, 6 h (stage III); 130 °C temperature.

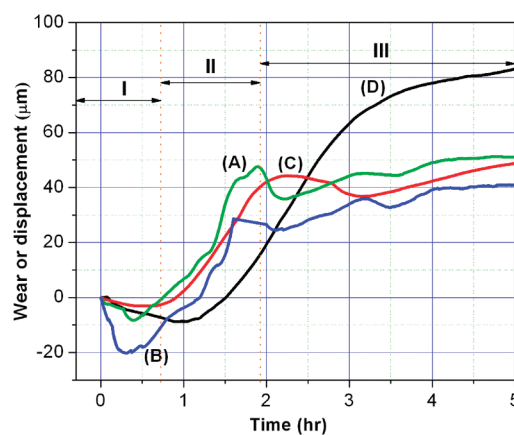


**Figure 9.** Wear (displacement) as a function of time using hexadecane without additive at 130 °C. (A) Fresh oil, fresh disk; (B) fresh oil, fresh disk; (C) fresh disk, oil oxidized for 10 h in experiment A, (D) Fresh oil, disk slid for 10 h in experiment B.

Figure 6 shows that not only the negative displacement of stage I is fully nullified in stage II, for example after 30 min of sliding ( $T = 120$  and 130 °C) in stage II, the positive displacement continues for another 1 h of sliding. Toward the latter part of this time span the rate of positive displacement reduces gradually with time. After about 3 h of sliding, the rate of displacement is reduced to less than half of that which exists at the beginning of stage II. This marks the beginning of stage III.

The exact mechanism that determines the rate of pin displacement in stage II requires further investigation. The observations presented above however indicate simultaneous existence of a number of mechanisms such as dissolution/wear/stripping of stage I deposits, generation of reactive secondary products of oil oxidation, formation of iron-carboxylate soap and metal to metal



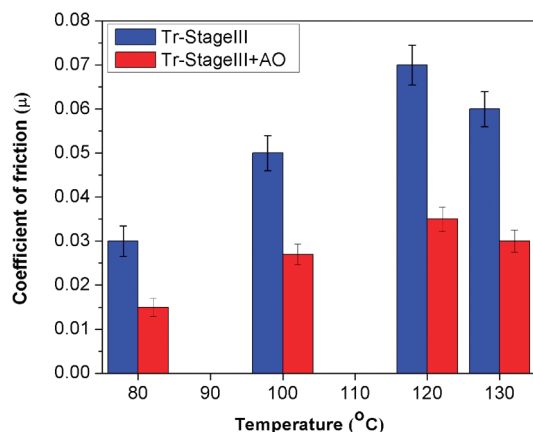


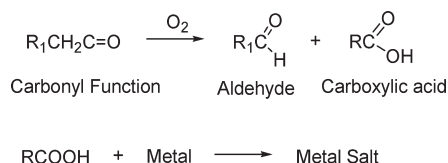
**Figure 10.** Coefficient of friction in stage III of tribo-oxidation of hexadecane, with and without additive. The bars show typical scatter in the data (one standard deviation).

contact, all of which contribute in varying degrees to result in the pin displacement characteristics seen in Figure 6.

On the basis of these observations, we may suggest that two principal mechanisms compete with each other in this stage. The organic secondary products generated react with iron of the pin and disk to raise a tribofilm which consists of iron carboxylate and other secondary products of oil oxidation. Initially the film is thin, allowing metal to metal contact and rapid wear. With time the film become thicker and a near equilibrium state is established at the end of stage II where the rates of film generation and film removal are about to same and a stable film controls the tribolayer. The stage II pin displacement characteristic, however, is dependent on the initial condition of the interfaces. If a thick deposit for example is made to exist at the commencement of stage I by using a pin and a disk already slid for 10 h and the experiment is run with fresh oil, the stage II pin displacement rate is reduced and the time required to equilibrate is increased. The characteristic curves A, B, and C in Figure 9 correspond roughly to the same interfacial conditions where there is no tribofilm at the commencement of sliding. The characteristic curve D carries a thick film at the commencement of the interaction.

**Stage III.** Stage III shows (Figure 6) a wear rate that is almost invariant with time, temperature, and the presence of antioxidant in the oil. This positive wear rate is significantly lower than what is achieved in stage II.

Figure 4c shows the XPS spectra of the pin surface after 9 h of sliding. The bonds detected are as indicated in the figure. The presence of a small amount of FeS was confirmed by taking a  $S_{2p}$  spectrum (not shown). Compared to the spectrum corresponding to stage II, the stage III pin surface shows a distinct carboxylic bond



Such metal salts are known to be catalytic for further oxidation of oil.<sup>10</sup> Compared to what is observed on the pin surface in stage II (Table 2), Table S2 (see the Supporting Information) shows enhanced presence of carbon and a diminished presence of iron

and oxygen. This suggests the presence of a thick and adherent organic film on the pin surface. The corresponding pin surface (Figure 7e,f) is smooth and shows minimal evidence of attrition. EDS of the debris generated in stage III after 9 h of sliding gives C:O:Fe ratios as 3.57:1:1.5, indicating the possibility that the debris particles are covered by a thin layer of carboxylate. The pin subsurfaces (Figure 8 c and d) show minimal plastic flow and the presence of a 40–60 nm thick tribolayer. Figure 10 shows the friction coefficient recorded in stage III at the end of 10 h of sliding time. The antioxidant is seen to reduce the friction significantly from that recorded in experiments without antioxidants.

## 4. CONCLUSIONS

The present work demonstrates that when hexadecane is used as a lubricating oil it ages considerably faster than what is observed by auto-oxidation. This difference has been demonstrated to be due to the catalytic action of iron. When no antioxidant is dispersed in oil, the time frame for the generation and depletion of hydroperoxide, the core reactant of the oil oxidation process is shown to shift from 8–12 h in auto-oxidation to 1–4 h in tribo-oxidation. An important finding of the present work is that the nonsteady state phase of the wear process is also confined to within 1–2.5 h of sliding time since commencement. Unlike in the case of auto-oxidation, the impact of antioxidant on the aging of oil used for lubricating steel on steel sliding contact, is minimal. The antioxidants however have a major influence in building up a protective antiwear tribofilm of oxide and sulfide in the first 1 h of running. Oil oxidation does not influence friction and wear in the first one hour of running. We believe that friction and wear in the next transient stage of 1–2 h is influenced by oil oxidation. We believe that two competing mechanisms: (i) wear of the oxide and sulfide layers on the pin surface, and (ii) generation of a thin organic tribofilm on the pin surface due to oil oxidation, happen simultaneously in this stage. With time, the tribofilm thickness increases until the two processes equilibrate. Although the kinetics that govern the pin displacement in this stage require further investigation, the equilibrium marks the existence of a thick tribofilm that carries liquid hydrocarbon and secondary products of oxidation in contact with an adsorbed carboxylate soap on the metal surface. When this equilibrium is reached, stage III of pin displacement is initiated. The wear rate of the pin compared to that in the previous stage is halved. A very low rate of wear continues to hold over the present test duration of 12 h. This stage of the sliding interaction also yields a low-friction regime where the decomposed products of oil and disulfide react with metal to produce beneficial salts.

## ■ ASSOCIATED CONTENT

**S Supporting Information.** Additional technical information, including FTIR, GC-MS, EDS, and XPS analytical results (PDF). This material is available free of charge via the Internet at <http://pubs.acs.org/>.

## ■ AUTHOR INFORMATION

### Corresponding Author

\*Phone: +918022932589. Fax: +918023600648. E-mail: [skbis@mecheng.iisc.ernet.in](mailto:skbis@mecheng.iisc.ernet.in).

## ACKNOWLEDGMENT

The authors are grateful to the General Motors (R&D) Warren, MI, for providing the financial support that has made this work possible. We acknowledge the help given by Mr. Anirban Mahato and Mr. H. S. Shamasunder of the IISc, in carrying out this work. We gratefully acknowledge our discussion related to this work with Prof. Colin D. Bain of the University of Durham, U.K..

## REFERENCES

- (1) Jensen, R. K.; Korcek, S.; Mahoney, L. R.; Zinbo, M. *J. Am. Chem. Soc.* **1979**, *101*, 7574–7584.
- (2) Jensen, R. K.; Korcek, S.; Mahoney, L. R.; Zinbo, M. *J. Am. Chem. Soc.* **1981**, *103*, 1742–1749.
- (3) Tseregounis, S. I.; Spearot, J. A.; Kitet, D. J. *Ind. Eng. Chem. Res.* **1987**, *26*, 886–894.
- (4) Blaine, S.; Savage, P. E. *Ind. Eng. Chem. Res.* **1991**, *30*, 92–798.
- (5) Blaine, S.; Savage, P. E. *Ind. Eng. Chem. Res.* **1991**, *30*, 2185–2191.
- (6) Blaine, S.; Savage, P. E. *Ind. Eng. Chem. Res.* **1992**, *31*, 69–75.
- (7) Ofunne, G. C.; Maduako, A. U.; Ojinnaka, C. M. *Tribol. Int.* **1991**, *24*, 173–178.
- (8) Adhvaryu, A.; Perez, J. M.; Singh, I. D.; Tyagi, O. S. *Energy Fuels* **1998**, *12*, 1369–1374.
- (9) Pullabhotla, V. S. R. R.; Southway, C.; Jonnalagadda, S. B. *Catal. Commun.* **2008**, *9*, 1902–1912.
- (10) Cochran, G. J.; Rizvi, S. Q. A. In *Fuels and Lubricants Handbook: Technology, Properties, Performance, and Testing*; Totten, G. E., Westbrook, S. R., Shah, R. J., Eds.; ASTM International: West Conshohocken, PA, 2003; Manual Series: MNL37WCD, p 787.
- (11) Plaza, S.; Mazurkiewicz, B.; Gruzinski, R. *Wear* **1994**, *174*, 209–216.
- (12) Plaza, S. *ASLE Trans.* **1987**, *30*, 493–500.
- (13) Kajdas, C.; Makowska, M.; Gradkowski, M. *Lubr. Sci.* **2003**, *15*, 329–340.
- (14) Makowska, M.; Kajdas, C.; Gradkowski, M. *Tribol. Lett.* **2002**, *13*, 65–70.
- (15) Ma, Y.; Liu, J.; Zheng, L. *Tribol. Int.* **1995**, *78*, 329–334.
- (16) Hsu, S. M.; Klaus, E. E. *ASLE Trans.* **1977**, *22*, 135–145.
- (17) Schneider, E. W. *Development of an Engine Dynamometer Test for Rapid Evaluation of Engine Oil Degradation under High-Temperature, High-Load Conditions*; Society of Automotive Engineers International: Warrendale, PA, 2005; SAE Paper 2005-01-3821.
- (18) Colclough, T. *Ind. Eng. Chem. Res.* **1987**, *26*, 1888–1895.
- (19) Naidu, S. K.; Klaus, E. E.; Duda, J. L. *Ind. Eng. Chem. Prod. Res. Dev.* **1988**, *25*, 596–603.
- (20) Lax-pent, C.; Patin, H. J. *Mol. Catal.* **1992**, *72*, 315–329.
- (21) Lara, J.; Blunt, T.; Kotvis, P.; Riga, A.; Tysoe, W. T. *J. Phys. Chem. B* **1998**, *102*, 1703–1709.
- (22) Forbes, E. S.; Reid, A. J. D. *ASLE Trans.* **1972**, *16*, 50–60.